Reaction Chemistry & Engineering

ROYAL SOCIETY OF CHEMISTRY

MINI REVIEW

View Article Online
View Journal

Cite this: DOI: 10.1039/d4re00384e

A mini review on aromatization of *n*-alkanes

Hongqi Wang and N. Raveendran Shiju *

Received 5th August 2024,
Accepted 19th October 2024

DOI: 10.1039/d4re00384e

rsc.li/reaction-engineering

The catalytic aromatization of *n*-alkanes is an important process in the chemical industry, especially for the production of value-added aromatics from the abundant and unreactive small alkanes. This mini review summarizes the recent progress on the development of catalysts for the aromatization of *n*-alkanes and the mechanistic studies. The effects of various catalysts (*e.g.* shape selective zeolites and noble metals) and reactant compositions on the aromatization performance are discussed to shed light on the rational design of novel heterogeneous catalysts.

1. Introduction

The catalytic aromatization of *n*-alkanes is an important process to upgrade the low-cost feedstock into value-added aromatic chemicals such as benzene, toluene and xylene (BTX) and to improve the octane number of gasoline.[1–3] The abundant alkanes could be acquired from the traditional fossil fuels (*e.g.* crude oil and natural gas, especially shale gas), as well as from recycled sources (*e.g.* chemical degradation of plastic waste). Catalytic aromatization is one of the most promising methods to valorize these alkanes.[4] The produced aromatic compounds, especially BTX, are crucial building blocks in the chemical industry, and currently BTX is mainly produced from naphtha reforming.[5] Another advantage of alkane aromatization, especially for utilizing methane and ethane, is the easier transportation of the liquid-form aromatic compounds than the feedstock gases.

Alkane aromatization is generally composed of complicated multi-step reactions in parallel or series over a catalyst, including cracking, dehydrogenation, isomerization, oligomerization and cyclization reactions.[6] Various parameters, including the reactant composition, catalyst and operating parameters (*e.g.* temperature and pressure), will affect the reaction routes and thus the product distribution and yield. Among these factors, the reactant and catalyst are of paramount importance and would be discussed in this review. Among the reactants, the aromatization of CH_4 and C_2H_6 is still in the laboratory developmental stage. However, for C_{3+} alkanes, some aromatization processes are commercial, such as Cyclar (UOP and BP) and M2-reforming (Mobil). The Zeolite Socony Mobil-5 (ZSM-5) zeolite and its various modifications (*e.g.* gallium modified) are effectively utilized in these processes due to their shape selectivity and ability to inhibit coke formation.[7] However, almost all the aromatization processes are limited by their low yield because of side reactions and catalyst deactivation due to coke formation.[8] Various new catalysts are developed to overcome these bottleneck problems by improving the activity, selectivity and long-term stability.

While there are some reviews focusing on certain alkanes (*e.g.* naphtha[3]) or catalysts (*e.g.* ZSM-5 (ref. 9)), a generalized mechanism is necessary to understand the interaction between alkanes and catalysts. This review summarizes the recent advances of the catalyst development and discusses the effects of the reactant composition during the catalytic aromatization of linear alkanes, aiming to provide readers a comprehensive insight into the generalized mechanism of alkane aromatization (especially the importance of an unsaturated intermediate pool) and to give a perspective about future direction. Firstly, zeolite catalysts together with their modifications, noble metals and other types of catalysts are summarized. Then the effects of reactants including single alkanes, co-aromatization and process coupling with oxidation are also discussed.

2. Catalysts

2.1. Zeolites

2.1.1. Unmodified zeolite. Zeolites are the most commonly utilized catalysts for alkane aromatization due to their shape selectivity and ability to reduce coke formation. The H-ZSM-5 zeolite is the most widely used framework type for alkane aromatization. Besides the framework structure, the type of acidity and strength determined by heteroatom species (*e.g.* Al or Ga) and the ratio of the heteroatom to Si also affect the catalytic performance for alkane aromatization. In addition, the smaller crystal size of H-ZSM-5 catalysts leads to enhanced cracking activity to form olefins because the larger external surface allows more pore entrances.[10] The cracking

Catalysis Engineering Group, Van't Hoff Institute for Molecular Sciences, University of Amsterdam, 1090 GD Amsterdam, The Netherlands. E-mail: h.wang4@uva.nl, n.r.shiju@uva.nl

reaction is favored on Brønsted acid sites compared to dehydrogenation during the conversion of alkanes when using unmodified (monofunctional) zeolite catalysts.[11] The initial activation of alkanes is generally the rate determining step, which could convert the unreactive alkanes into adsorbed olefin species. The cracking and dehydrogenation mechanisms correspond to the C–C bond cleavage and C–H bond activation, respectively. These cracking products, especially the unsaturated olefin species on the acid sites, might be the intermediates for the subsequent aromatic formation.[12] The internal channels or pores of the zeolites could help the conversion of the activated intermediates to aromatics through oligomerization, cyclization and dehydrogenation (Fig. 1).

2.1.2. Metal modified zeolites. To improve the selectivity to aromatics, many metal elements such as Ga, Zn, Pt, Mo, Mg and Cu are utilized to modify the zeolite to produce bifunctional catalysts.[9,13–18] Generally, the Brønsted acid sites of unmodified zeolites (section 2.1.1) would contribute to the cracking reaction, whereas the introduction of metal elements could lead to the formation of Lewis acid sites which would enhance the dehydrogenation reaction. In other words, the Brønsted acid sites would favor the C–C bond breakage, while the Lewis acid sites would promote C–H bond cleavage during the activation of the reactant alkane. As shown in Fig. 2, the cracking rate is higher than the dehydrogenation rate on Brønsted acid sites (Ga/Al = 0), whereas the dehydration rate is higher than the cracking rate on Lewis acid sites (Ga/Al > 0).[19] The introduction of metal elements into the zeolite can create Lewis acid sites which can promote the dehydrogenation. For example, the dehydrogenation rate of *n*-butane over Ga/H-MFI is 180 times higher than that over H-MFI under the same conditions.[20] Both Lewis and Brønsted acid sites are involved in the aromatization process, especially for ethylene oligomerization.[21] It is also reported that alkane dehydrogenation can also occur over Lewis–Brønsted acid site pairs *via* a bifunctional mechanism derived from the synergy between the Lewis and Brønsted acid sites.[19] Therefore, the Brønsted and Lewis acidity of the zeolite catalyst could be tuned to optimize the catalytic performance. Pyridine Fourier transform infrared spectroscopy (FT-IR) is usually utilized to quantify the Brønsted and Lewis acid sites.[22]

The nature and dispersion of the metal modifier have an impact on the activity, which could be tuned by preparation

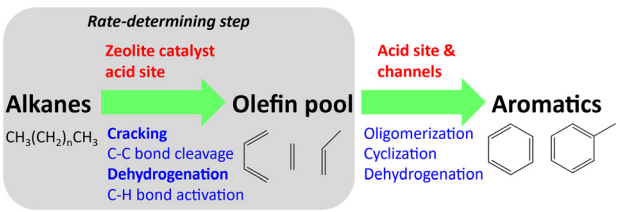

Fig. 1 Generalized steps for the catalytic aromatization of alkanes on zeolite catalysts.

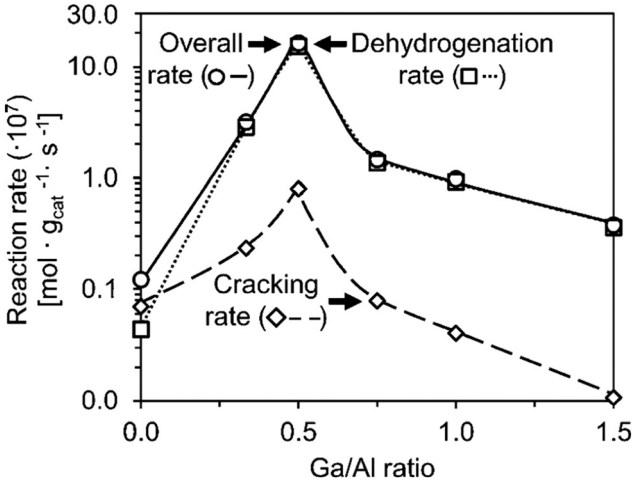

Fig. 2 Cracking and dehydrogenation rates at different Ga/Al ratios (this figure is reproduced from ref. 19 with permission).

and pretreatment methods. For example, it is reported that Zn^{2+} on H-BEA zeolite prepared by a reaction with zinc vapor has higher activity than ZnO/H-BEA synthesized by hydrolysis of zinc–organic species during propane aromatization.[23] However, in another study, the opposite conclusion was reached indicating that subnanometric ZnO clusters on H-ZSM-5 might have higher selectivity than Zn^{2+} ions.[24] This contradictory result might be caused by a support effect. For example, a Zn/SiO_2@ZSM-5 core–shell catalyst synthesized by a hydrothermal coating method would lead to higher alkane conversion and aromatic selectivity than the conventional Zn/ZSM-5 during the co-aromatization of methane and propane.[25] Moreover, H_2-chemisorbed Zn species could significantly improve the aromatic selectivity to 30% by hydrogen treatment compared to 11% of H-ZSM-5 during pentane aromatization.[26] Additionally, it is found that a Zn/ZSM-5 microsphere catalyst with a hierarchical structure exhibited improved stability compared to the conventional microporous Zn/ZSM-5 because of the presence of intergranular mesopores which could enhance the molecular transport and resistance to coke formation.[27]

Furthermore, Zn and Pt are commonly used as promoters for alkane reforming to achieve high BTX yields due to the incorporation of Zn into the framework of ZSM-5 and the enhanced metal dispersion by Pt.[1,5,28] It is reported that Zn, as a promoter, can increase the aromatic selectivity.[29] Similarly, Pt could enhance the catalytic conversion of ethane because of the strengthened reducibility of Ga species on ZSM-5 (ref. 30) and the synergistic interaction.[31] One disadvantage of Zn/ZSM is the agglomeration and loss of Zn after a certain time on stream even though it could be re-dispersed evenly after regeneration.[29,32] Zn/ZSM-5 should be modified with higher thermal stability and activity, such as introducing other metal elements.

Similarly, the Lewis acid sites of Ga modified zeolite promoted the aromatization, and Ga introduced by direct (or *in situ*) synthesis seemed to have better performance.[31,33] The

GaH_2^+ species was highly active for hexane dehydroaromatization over Ga modified H-ZSM-5 and could be acquired by pretreatment using hydrogen.[34] The Ga species incorporated in the framework favored the BTX formation than the extra framework ones because of the insignificant shielding of acid sites for the framework ones.[35] As for the effects of dispersion, the highly dispersed Ga on hierarchical zeolite nanosheets also contributed to the activation of *n*-pentane.[36] However, the mesopores of desilicated hierarchical Ga/H-ZSM-5 *via* alkaline treatment decreased the activity and selectivity for propane aromatization apparently because the mesopores lowered the residence time of olefins and inhibited the dehydrogenation which is the rate-determining step.[37] The investigation of structure–activity relationships by correlating the catalyst structure and performance could give some insights into the reaction pathway, which also emphasizes the importance of the olefin pool shown in Fig. 1.[38] In addition, *operando* characterization is required to analyse the active sites even though the coke formation could make the analysis difficult.[39]

Mo-modified zeolite can be used to aromatize small alkanes (*e.g.* C1–C3).[18] The induction period is consistently present when using Mo/ZSM-5.[40] This is because Mo carbide as the active species will be formed by carburization at the beginning.[41] Mg as a promoter can enhance the catalytic activity and stability of Mo/ZSM-5.[42]

High Cu loading decreases the acidic strength of the zeolite catalyst, which can maintain the alkane conversion and selectivity to aromatics.[13] It is reported that mononuclear Cu is the dominant species at low Cu loading (0.1 wt%), while multinuclear Cu with a Cu–O–Cu bridge is the main species at higher Cu loading (1.4 wt%).[43]

2.1.3. Non-metal modification. Phosphorus (P) is a typical non-metal modifier for alkane aromatization catalysts. The introduction of P can form aluminum phosphate with both framework and extra-framework Al and thus can decrease the concentration and strength of Brønsted acid sites over the parent H-ZSM-5.[44] Besides reducing the strength of acid sites, the P modification could also tune the pore structure of zeolite, which would help decrease the H_2 formation barriers and promote the formation of aromatics.[45] For example, P could enhance the yield of liquid aromatics and stability in ethane conversion as shown in Fig. 3. Additionally, the P modification improved the hydrothermal stability of Ga-ZSM-5 by lowering the binding energy between H_2O and the Brønsted acid sites and decreased the coke formation by reducing the amount of strong acid sites where cracking is favored.[45]

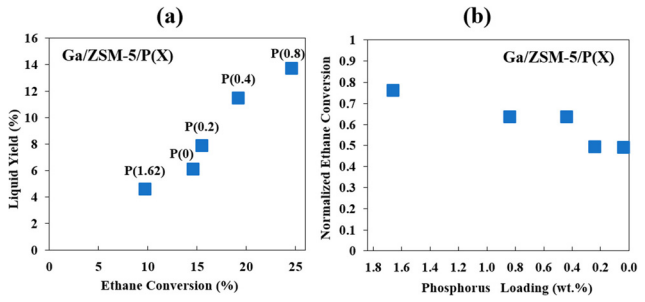

Fig. 3 Effects of phosphorus (wt%) on the yield of liquid aromatics (a) and ethane conversion (b) (this figure is reproduced from ref. 45 with permission).

Similar to phosphorus, boron, being near to Al and Si in the periodic table, could also reduce the deactivation rate in a Zn–B/ZSM-5 catalyst during hexane aromatization even though it decreased the catalyst activity initially.[46] Boron was incorporated into the framework and reduced the acidity of the Brønsted acid sites, which could further limit the conversion of coke precursors on these sites.

2.2. Noble metals

Noble metal catalysts such as platinum and palladium[47] are generally featured with high activity and are extensively applied on the scale of single atoms, clusters and nanoparticles loaded on various supports such as carbon, zeolite and alumina. Table 1 shows various catalyst combinations and their performance. A single site platinum catalyst on a CeO_2 support exhibited high selectivity for dehydrocyclization and aromatization reactions compared to Pt cluster and nanoparticle catalysts during hexane reforming even though its thermal stability degraded after 450 °C.[48] Besides the noble metal sizes, the location of the metal atoms on the support could also affect the catalyst performance and therefore the product distribution. For example, the Pt nanoparticles inside the zeolite channels led to higher selectivity to aromatics than those on the external surface because the Pt sites inside the pores would favor the cyclization.[49] However, the Pt particles inside the channels might relocate to the outside during the reaction and thus lead to deactivation.[50] Besides the relocation of Pt particles, the higher cost of noble metals than Ga and Zn should also be taken into consideration. The development of single atom noble metal catalysts may help to decrease the cost due to the maximum utilisation of noble metals.[48]

The catalytic performance of noble metal catalysts is also support-dependent. The hierarchical support structure (*e.g.* micro-/mesoporous Pt/KL) can enhance the aromatization by a combined effect of the high activity of Pt in micropores and the inhibited side reactions due to the mesoporous catalyst.[52] For example, the mesopores in Pt/desilicated ZSM-5 contributed to the higher ethane conversion by 60% and BTX selectivity by 75% compared to the Pt/conventional ZSM-5.[51] Some macroporous oxide (*e.g.* Ta_2O_5) supports can improve the desired selectivity (up to 97% towards isomerization) by allowing charge transfer at the metal–oxide interface and high electron density of Pt.[53]

Furthermore, metal promoters such as Zn[54,55] and Fe[56] could be introduced to improve the dispersion of noble metal atoms on the support. The formed bimetallic catalyst enhanced the alkane conversion and BTX selectivity by

Table 1 Noble metal catalysts for the aromatization of alkanes

Noble metal	Support	Reactant	Conditions	Conversion/selectivity	Key findings	Ref.
Pd	C	*n*-Octane	500 °C, WHSV = 2 h^{-1}, hydrogen to hydrocarbon molar ratio = 2	Conversion = 54.4 wt%; aromatic selectivity = 58 wt%	Pd/C has higher selectivity to xylenes	47
Pt	CeO_2	*n*-Hexane	500 °C	Conversion = 5%; aromatization selectivity = 40%	The single-site catalyst Pt/CeO_2 shows higher selectivity to dehydrocyclization and aromatization than CeO_2-supported Pt clusters and nanoparticles	48
Pt	KL zeolite	*n*-Heptane	420 °C, hydrogen/*n*-heptane molar ratio = 6, WHSV = 0.68 h^{-1}	Conversion = 88 mol%; aromatic selectivity = 84.3 mol%	The location of Pt nanoparticles in KL zeolites could be controlled by changing the exposure time of the Pt precursor	49
Pt	KL zeolite	*n*-Heptane	500 °C, 1 atm, WHSV = 1 h^{-1}, H_2/*n*-heptane = 6 mol mol^{-1}, Pt loading = 0.6 wt%	Conversion = 63.89 wt%; aromatic selectivity = 58.84 wt%	High dispersion of Pt in KL zeolite could improve the stability	50
Pt	Desilicated ZSM-5	Ethane	550 °C, 2 barg, GHSV = 0.3 h^{-1}	Conversion = 25%; selectivity = 42%	Pt nanoparticles in desilicated ZSM-5 are near the acid sites, which could increase the activity and selectivity to BTX	51

accelerating the initial dehydrogenation to form olefins and the subsequent dehydrocyclization to produce aromatics. Another study showed that the introduction of Zn to Pt over H-ZSM-5 could reduce the coke yield from 8.3 to 1.7 μg g_{cat}^{-1} h^{-1} and thus alleviate catalyst deactivation.[57] Moreover, for bimetallic catalysts, the interaction between both metals (*e.g.* Pt–Zn nanoparticles) and the support (*e.g.* uniform compact cylindrical ZSM-5) also improved the selectivity over 90% towards aromatics compared to the selectivity of less than 40% from Pt–Zn over the conventional ZSM-5.[58]

2.3. Other catalysts

Besides the widely-utilized zeolites and noble metals, other catalysts were also used to aromatize alkanes. GaN as a nitride semiconductor could catalyze the aromatization of light alkanes to benzene with high selectivity.[59,60] However, the small surface area (*e.g.* 8 m^2 g^{-1}) of GaN required high temperature (>650 °C) to initiate benzene formation because the activity is limited by the number of active sites which are dependent on the surface area.[3] Activated carbon doped with phosphorus is also reported to aromatize *n*-hexane into benzene with the –P(O)(OH) functional group as the active site.[61,62] The active sites of the P@AC catalyst are weak/medium-strength acidic centers in nature, which could selectively activate the C–H bond instead of the C–C bond.

2.4. Catalyst deactivation

During the catalytic aromatization of *n*-alkanes, coke formation is almost inevitable and is the major reason for the catalyst deactivation because the formed coke will block the active sites and zeolite channels.[63,64] However, measures could be taken to suppress the coke formation, such as developing bimetallic catalysts. Incorporation of Co into Mo/ZSM-5 could enhance the resistance to deactivation by reducing the coke formation during the aromatization of methane.[65] Similarly, introduction of Pt into Ga/ZSM-5 could facilitate the hydrogenolysis of coke precursors.[66] Besides modifying the catalyst, conducting aromatization under a reduction environment (*e.g.* with H_2 in the feed) could also suppress coke formation.[21,67]

3. Reactants

The aromatization of methane,[64] ethane,[7] and propane[68] has been separately reviewed in the literature. The purpose of discussion here is to provide a big picture about the influence of the alkane structure and a generalized reaction mechanism of alkane aromatization.

3.1. Single alkanes

CH_4 is abundant in natural gas and is produced as a by-product in many chemical processes. The strong C–H bond in CH_4 makes it the most unreactive hydrocarbon species. The most widely investigated catalyst for CH_4 aromatization is Mo/H-ZSM-5.[64] As shown in Fig. 1, the aromatization of CH_4 over Mo/H-ZSM-5 at 700 °C involves the formation of a hydrocarbon pool. An induction period was also observed due to the accumulation of adsorbed hydrocarbons on the Mo sites.[69] It is believed that the molybdenum carbide species are only responsible for the activation of CH_4 molecules and Mo-carbide/H-ZSM-5 is more active and stable than Mo-oxide/H-ZSM-5 during CH_4 aromatization.[70,71] This could explain the presence of an induction period when the Mo-oxide is converted into Mo-carbide. The formation of carbides is facilitated by the reduction and carburization pretreatment and thus improved the catalytic properties.[72] As shown in Fig. 4, the catalysts with pre-carburization demonstrated a higher benzene yield and a slower deactivation rate. Various Mo-carbide species such as MoC,[39] Mo_2C,[73] Mo_2C_6,[74] and MoC_xO_y,[75] each with distinct structural and catalytic properties, may be the active sites to catalyze

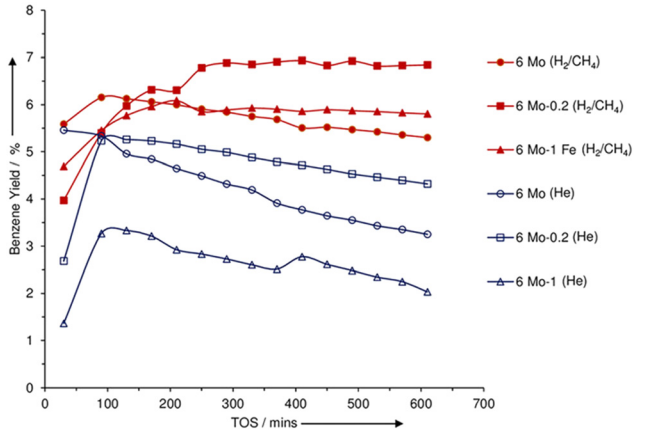

Fig. 4 Benzene yield for 6Mo/ZSM-5, 6Mo-0.2Fe/ZSM-5, and 6Mo-1Fe/ZSM-5 catalysts under He treatment (open symbols) and pre-carburization (closed symbols) (this figure is reproduced from ref. 72 with permission).

the aromatization. There is still debate about the evolution of the species during the reaction and their effects on the catalytic performance. For instance, it is reported that the isolated Mo-oxide evolves into Mo-carbide nanoparticles during the reaction.[76] It is also proved that even though MoC_xO_y could activate CH_4, MoC_x is essential for the formation of aromatics.[75] To resolve the debate, advanced *operando* techniques are required to determine the reaction pathways. In addition, the doping of metal elements such as Co and Pd to the Mo/ZSM-5 catalyst enhanced the stability and improved the resistance to deactivation.[65,73] It is also reported that the physical mixing of NiO with Mo/H-ZSM-5 enhanced the aromatic yield and catalytic stability because NiO could increase the dispersion of molybdenum carbide and metal Ni can decrease the coke formation by converting the coke precursors to carbon nanotubes.[41] Besides zeolite, sulfated zirconia supported Mo with various promoters could also promote the aromatization with little coke formation.[77]

Similar to the unreactive methane, ethane aromatization has not been commercialized until now as well. Besides Mo/ZSM-5 and its modification (*e.g.* Fe or Zn as the promoter),[29] other active metals such as Pt,[78] Zn,[21] Ga,[40] Re,[79] GaPt[30,66] and NiGa[80] could be supported on ZSM-5 to catalyze the ethane aromatization reaction. After ethane activation (*i.e.* dehydrogenation), oligomerization would also take place to form new C–C bonds over both Brønsted and Lewis acid sites.[81] The newly formed unsaturated intermediate pool of a certain size (*e.g.* C_6–C_8) would further undergo cyclization and dehydrogenation to produce aromatics.

The aromatization of C_{3+} alkanes, especially the C_3–C_6 species and their mixture, has been commercialized using a Ga or Zn modified H-ZSM-5 catalyst or supported noble metals, such as Cyclar and M2-reforming processes. Typically, the yield of aromatic compounds could reach up to 58–60 wt% when C_3 and C_4 are utilized as the feedstocks.[7] Lower temperature is generally required for the aromatization of C_{3+} alkanes compared to methane or ethane.[82]

The aromatization of C_{6+} alkanes is also called "reforming" in the industry. The main aim of reforming is to convert alkanes and cycloalkanes into aromatics with platinum catalysts such as Pt/γ-Al_2O_3 and Pt/KL zeolite.[83–86] Besides the supported noble metal catalysts, other metals such as Mo,[63] Cu,[13] and Ga[34] could also be utilized to achieve the aromatization. Even though it is thought that the straight carbon chain of C_6–C_8 alkanes could be converted into aromatics without cracking or oligomerization reactions,[58] BTX will be present in the products when a single alkane acts as the reactant,[87] which could prove the existence of the unsaturated intermediate pool.

The reports of the aromatization of C_{9+} alkanes are fewer than the lighter alkanes. The cracking reaction of C_{9+} alkanes would be more desired compared to the light alkanes,[12] because it would be easier for the C_2–C_8 species in the unsaturated intermediate pool to form the aromatics. After cracking, the species in the unsaturated intermediate pool would undergo a similar aromatization route.[88]

3.2. Co-aromatization

Co-aromatization is generally conducted for CH_4 with other alkanes such as propane[89,90] and pentane[91] because it is supposed that the presence of a co-reactant could reduce the thermodynamic limitation. Conversely, CH_4 could also function as a co-reactant to promote BTX production during the aromatization of light alkanes over Zn-Ga/H-ZSM-5 (ref. 92) or the aromatization of complex naphtha over Zn–Pt/H-ZSM-5.[28] As shown in Fig. 5, the presence of methane could increase the liquid and BTX yields compared to N_2. The H_x and CH_x intermediates formed from CH_4 are anticipated to participate in the formation of light aromatics and suppress the formation of heavy

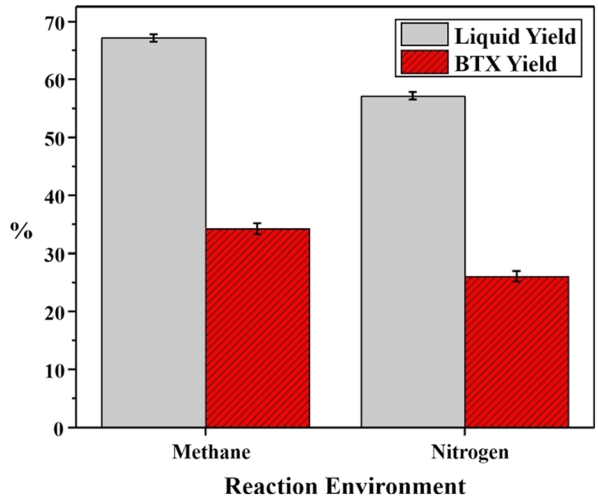

Fig. 5 Effects of environments on liquid and BTX yields during the reforming of naphtha utilizing a Pt–Zn/ZSM-5 catalyst (this figure is reproduced from ref. 28 with permission).

aromatics compared to N_2.[67] The incorporation of fragments from CH_4 in the products during the co-aromatization with propane was supported by the detection of ^{13}C of CH_4 in the aromatic rings of the products.[93,94] The catalyst properties might affect the CH_4 reaction pathway, such as the acidity influenced by the Al sites[95] and the location of Zn species over the Zn/H-ZSM-5 zeolite.[96] The aromatization of naphtha as a paraffin mixture could also be considered as co-aromatization of similar alkanes.[97]

3.3. Coupling with the oxidation process

Besides the direct aromatization discussed above, oxidative dehydrogenation could be coupled with aromatization. CO_2 has been used already to produce valuable olefins or synthesis gas from alkanes *via* CO_2-oxidative dehydrogenation (CO_2-ODH) or dry reforming.[98–100] Chen *et al.* proposed a tandem CO_2 oxidative dehydrogenation–aromatization reaction, which could promote the dehydrogenation and enhance the subsequent aromatization by consuming H_2.[45] Fig. 6 demonstrates that CO_2-oxidative dehydrogenation and aromatization could achieve a higher equilibrium ethane conversion than direct dehydrogenation and aromatization. It is proposed that CO_2 consumes the coke *via* the reverse Boudouard reaction ($CO_2 + C \rightarrow 2CO$), thus enhancing stability.[101] Moreover, the reverse water gas shift reaction (RWGS) is promoted by CO_2, consuming H_2 and thereby enhancing the dehydrogenation activity.

Besides the direct coupling of chemical reactions, the methane aromatization process can also be integrated with the chemical looping for selective H_2 oxidation and H_2O removal so that a high combined aromatic yield could be acquired for the whole integrated process.[102]

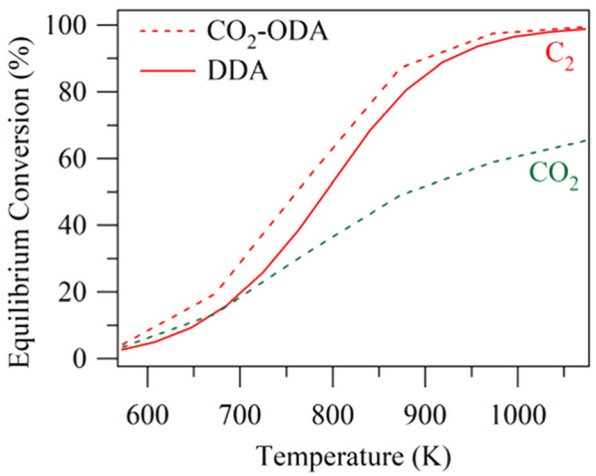

Fig. 6 Effects of temperature on the equilibrium ethane conversion (DDA: direct dehydrogenation and aromatization; CO_2-ODA: CO_2-oxidative dehydrogenation and aromatization) (this figure is reproduced from ref. 45 with permission).

4. Challenges and outlook

During the catalytic aromatization, low activity/selectivity especially for methane conversion and catalyst deactivation are the main challenges.[29] As discussed in section 3.1, methane is very difficult to activate, which requires high temperatures. On the other hand, elevated temperatures could cause side reactions that lower the selectivity and increased coke formation accelerating the deactivation. Promising catalysts are reported in the literature; however, improvements are still needed in activity and stability. Moreover, the scale-up should be carefully considered, as most of the studies are on a lab-scale. Alternate reactor configurations also need to be studied, considering the heat effects associated with the reaction.

Future efforts should be focusing on using small alkanes such as methane from abundant natural gas[7] and carbonous waste such as biomass and plastic waste. New catalysts and process technologies need to be developed to address the challenges, as mentioned above.[23]

Conclusions

This paper reviews the recent advances about the development of catalysts and the mechanism investigations of alkane aromatization. The most important step in the alkane aromatization is the activation of alkanes to form an unsaturated intermediate pool with the help of a catalyst. The C–H bond activation is essential for the formation of an unsaturated intermediate pool from the alkanes, whereas the C–C bond breakage would occur *via* cracking. For zeolite catalysts, Brønsted acid sites favor the C–C bond breakage while Lewis acid sites promote C–H bond cleavage during the activation of the reactant alkane. Oligomerization might also occur depending on the exact carbon number of the alkane feedstock, such as methane and ethane, which are more difficult to activate compared to higher alkanes. Besides zeolites and their modified materials, noble metals and other catalysts such as GaN could also be utilized to aromatize alkanes. Based on the summary of the past studies, we believe that there is still a large scope for future research in different aspects of this reaction. There is potential in either improving the existing catalysts or designing new catalysts which could enhance the formation of the unsaturated intermediate pool. The use of predictive modeling or a rapidly developing machine learning approach may help to identify novel potential compositions that were not tested so far in this reaction.[103] Materials such as niobia, whose Lewis/Brønsted acidity is tunable, could also be examined as part of such compositions.[104–106] It would also be interesting to try non-conventional synthesis methods such as hydrothermal methods and microwave-assisted methods to accelerate the catalyst synthesis or to control the compositions more accurately.[107] Doping with suitable components will also help to modulate the activity and stability of the new catalyst compositions.[108]

The use of tandem reactions, as described above, could be another option to overcome the issues in the direct aromatization such as coke deposition and consequent deactivation. It would also help in having a deeper insight into the mechanism through *in situ* spectroscopy and computational calculations. Simultaneously, studies in the reaction engineering will help to address the probable challenges in the potential scale-up possibilities of the aromatization of alkanes.

Data availability

No primary research results, software or code have been included and no new data were generated or analysed as part of this review.

Author contributions

Hongqi Wang: conceptualization, investigation, data curation, visualization, writing – original draft, writing – review & editing. N. Raveendran Shiju: supervision, writing – review & editing.

Conflicts of interest

There are no conflicts to declare.

References

1 Q.-M. Zhou, S. Wang, Z.-F. Qin, M. Dong, J.-G. Wang and W.-B. Fan, *J. Fuel Chem. Technol.*, 2023, **51**, 1529–1539.
2 K. Li, M. Yan, H. Wang, L. Cai, P. Wang and H. Chen, *Fuel Process. Technol.*, 2023, **252**, 107982.
3 M. N. Akhtar, A. M. Aitani, A. C. Ummer and H. S. Alasiri, *Energy Fuels*, 2023, **37**, 2586–2607.
4 F. Yu, S. Liu and B. Liu, *Molecules*, 2024, **29**, 1288.
5 D. Xu, L. Wei, M. Yan, F. Yi, G. Zhao, A. Jia, D. Zhu, S. Wang and Y. Li, *Appl. Catal., A*, 2023, **663**, 119308.
6 G. He and D. Mei, *J. Catal.*, 2024, **436**, 115623.
7 Y. Xiang, H. Wang, J. Cheng and J. Matsubu, *Catal. Sci. Technol.*, 2018, **8**, 1500–1516.
8 V. I. Bogdan, A. E. Koklin, I. I. Mishanin, T. V. Bogdan, N. V. Mashchenko and L. M. Kustov, *Mendeleev Commun.*, 2021, **31**, 230–232.
9 D. Liu, L. Cao, G. Zhang, L. Zhao, J. Gao and C. Xu, *Fuel Process. Technol.*, 2021, **216**, 106770.
10 A. A. Rownaghi, F. Rezaei and J. Hedlund, *Chem. Eng. J.*, 2012, **191**, 528–533.
11 T. F. Narbeshuber, H. Vinek and J. A. Lercher, *J. Catal.*, 1995, **157**, 388–395.
12 S. Pradhan, R. Lloyd, J. K. Bartley, D. Bethell, S. Golunski, R. L. Jenkins and G. J. Hutchings, *Chem. Sci.*, 2012, **3**, 2958–2964.
13 O. Tursunov, L. Kustov and Z. Tilyabaev, *J. Pet. Sci. Eng.*, 2019, **180**, 773–778.
14 C. M. Lok, J. Van Doorn and G. Aranda Almansa, *Renewable Sustainable Energy Rev.*, 2019, **113**, 109248.
15 F. Goodarzi, R. P. Thumbayil, K. Enemark-Rasmussen, J. Mielby, T. T. M. Nguyen, P. Beato, F. Joensen and S. Kegnæs, *ChemCatChem*, 2020, **12**, 1519–1526.
16 B. Xu, M. Tan, X. Wu, H. Geng, F. Song, Q. Ma, C. Luan, G. Yang and Y. Tan, *Fuel*, 2021, **283**, 118889.
17 Z. Hou, X. Mi, X. Li and H. Liu, *Ind. Eng. Chem. Res.*, 2021, **60**, 12100–12108.
18 Y. Hyun Lim, H. Won Ryu, K. Nam, Y. Hwang, J. Roh and D. Heui Kim, *Fuel*, 2023, **342**, 127906.
19 M. W. Schreiber, C. P. Plaisance, M. Baumgärtl, K. Reuter, A. Jentys, R. Bermejo-Deval and J. A. Lercher, *J. Am. Chem. Soc.*, 2018, **140**, 4849–4859.
20 N. M. Phadke, E. Mansoor, M. Head-Gordon and A. T. Bell, *ACS Catal.*, 2021, **11**, 2062–2075.
21 T. Liang, S. Fadaeerayeni, J. Shan, T. Li, H. Wang, J. Cheng, H. Toghiani and Y. Xiang, *Ind. Eng. Chem. Res.*, 2019, **58**, 17699–17708.
22 A. K. Panda, A. Alotaibi, I. V. Kozhevnikov and N. R. Shiju, *Waste Biomass Valoriz.*, 2020, **11**, 6337–6345.
23 S. S. Arzumanov, A. A. Gabrienko, A. V. Toktarev, Z. N. Lashchinskaya, D. Freude, J. Haase and A. G. Stepanov, *J. Phys. Chem. C*, 2019, **123**, 30473–30485.
24 L. Lin, J. Liu, X. Zhang, J. Wang, C. Liu, G. Xiong and H. Guo, *Ind. Eng. Chem. Res.*, 2020, **59**, 16146–16160.
25 G. Xu and X. Zhu, *Appl. Catal., B*, 2021, **293**, 120241.
26 S. Tamiyakul, T. Sooknoi, L. L. Lobban and S. Jongpatiwut, *Appl. Catal., A*, 2016, **525**, 190–196.
27 J. Wang, C. Liu, P. Zhu, H. Liu, X. Zhang, Y. Zhang, J. Liu, L. Zhang and W. Zhang, *New J. Chem.*, 2021, **45**, 18659–18668.
28 J. Jarvis, A. Wong, P. He, Q. Li and H. Song, *Fuel*, 2018, **223**, 211–221.
29 B. Robinson, X. Bai, A. Samanta, V. Abdelsayed, D. Shekhawat and J. Hu, *Energy Fuels*, 2018, **32**, 7810–7819.
30 A. Caiola, B. Robinson, X. Bai, D. Shekhawat and J. Hu, *Ind. Eng. Chem. Res.*, 2021, **60**, 11421–11431.
31 Y. Wang, A. Caiola, B. Robinson, Q. Li and J. Hu, *Energy Fuels*, 2020, **34**, 3100–3109.
32 R. Geng, Y. Liu, Y. Guo, P. Wang, M. Dong, S. Wang, J. Wang, Z. Qin and W. Fan, *ACS Catal.*, 2022, **12**, 14735–14747.
33 Y. Zhou, H. Thirumalai, S. K. Smith, K. H. Whitmire, J. Liu, A. I. Frenkel, L. C. Grabow and J. D. Rimer, *Angew. Chem., Int. Ed.*, 2020, **59**, 19592–19601.
34 A. Thivasasith, T. Maihom, S. Pengpanich, J. Limtrakul and C. Wattanakit, *Phys. Chem. Chem. Phys.*, 2019, **21**, 5359–5367.
35 B. J. Lee, J. H. Lee, D. H. Kim, Y. G. Hur and K.-Y. Lee, *Microporous Mesoporous Mater.*, 2021, **323**, 111243.
36 W. Wannapakdee, D. Suttipat, P. Dugkhuntod, T. Yutthalekha, A. Thivasasith, P. Kidkhunthod, S. Nokbin, S. Pengpanich, J. Limtrakul and C. Wattanakit, *Fuel*, 2019, **236**, 1243–1253.
37 M. Raad, S. Hamieh, J. Toufaily, T. Hamieh and L. Pinard, *J. Catal.*, 2018, **366**, 223–236.

38 Y. Wu, Y. Lv, R. Wang, L. Bao, Z. Zhang, D. Shi, A. Zhang, Y. Zhang, Q. Liu, Q. Wu, D. Shi, K. Chen, G. Jiang and H. Li, *Langmuir*, 2024, **40**, 11998–12008.
39 I. Vollmer, I. Yarulina, F. Kapteijn and J. Gascon, *ChemCatChem*, 2019, **11**, 39–52.
40 E. A. Uslamin, H. Saito, Y. Sekine, E. J. M. Hensen and N. Kosinov, *Catal. Today*, 2021, **369**, 184–192.
41 K. Nam, H. W. Ryu, M. Y. Gim and D. H. Kim, *Appl. Catal., B*, 2021, **296**, 120377.
42 H. W. Ryu, Y. H. Lim, W. Jung, K. Nam, Y. Hwang, J. E. Roh and D. H. Kim, *Chem. Eng. J.*, 2023, **467**, 143404.
43 A. A. Kolganov, A. A. Gabrienko, S. A. Yashnik, E. A. Pidko and A. G. Stepanov, *J. Phys. Chem. C*, 2020, **124**, 6242–6252.
44 W. Lin, Y. Song, L. Han, X. Yang, J. Liu and B. Peng, *Fuel*, 2021, **299**, 120890.
45 E. Gomez, X. Nie, J. H. Lee, Z. Xie and J. G. Chen, *J. Am. Chem. Soc.*, 2019, **141**, 17771–17782.
46 P. T. Huyen, V. D. Trinh, M. Teresa Portilla and C. Martínez, *Catal. Today*, 2021, **366**, 97–102.
47 M. Yin, R. H. Natelson, A. A. Campos, P. Kolar and W. L. Roberts, *Fuel*, 2013, **103**, 408–413.
48 S. Zhang, L. Chen, Z. Qi, L. Zhuo, J.-L. Chen, C.-W. Pao, J. Su and G. A. Somorjai, *J. Am. Chem. Soc.*, 2020, **142**, 16533–16537.
49 D. Xu, S. Wang, B. Wu, C. Huo, Y. Qin, B. Zhang, J. Yin, L. Huang, X. Wen, Y. Yang and Y. Li, *J. Catal.*, 2018, **365**, 163–173.
50 K. Li, Q. Chang, J. Yin, C. Zhao, L. Huang, Z. Tao, Y. Yun, C. Zhang, H. Xiang, Y. Yang and Y. Li, *J. Catal.*, 2018, **361**, 193–203.
51 F. Goodarzi, D. B. Christensen, F. Joensen, S. Kegnæs and J. Mielby, *Appl. Catal., A*, 2020, **592**, 117383.
52 K. Lee and M. Choi, *J. Catal.*, 2016, **340**, 66–75.
53 K. An, S. Alayoglu, N. Musselwhite, K. Na and G. A. Somorjai, *J. Am. Chem. Soc.*, 2014, **136**, 6830–6833.
54 P. He, Y. Chen, J. Jarvis, S. Meng, L. Liu, X.-D. Wen and H. Song, *ACS Appl. Mater. Interfaces*, 2020, **12**, 28273–28287.
55 G. Liu, J. Liu, N. He, S. Sheng, G. Wang and H. Guo, *J. Energy Chem.*, 2019, **34**, 96–103.
56 D. Xu, S. Wang, B. Wu, B. Zhang, Y. Qin, C. Huo, L. Huang, X. Wen, Y. Yang and Y. Li, *ACS Appl. Mater. Interfaces*, 2019, **11**, 29858–29867.
57 J. Jarvis, P. He, A. Wang and H. Song, *Fuel*, 2019, **236**, 1301–1310.
58 J. S. Jarvis, J. H. Harrhy, P. He, A. Wang, L. Liu and H. Song, *Chem. Commun.*, 2019, **55**, 3355–3358.
59 L. Li, X. Mu, W. Liu, X. Kong, S. Fan, Z. Mi and C.-J. Li, *Angew. Chem., Int. Ed.*, 2014, **53**, 14106–14109.
60 K. Dutta, L. Li, P. Gupta, D. P. Gutierrez and J. Kopyscinski, *Catal. Commun.*, 2018, **106**, 16–19.
61 Y. Li, H. Zhao, S. Chen, S. Bao, F. Xing and B. Jiang, *Catal. Commun.*, 2021, **156**, 106318.
62 Y. Li, S. Bao, H. Zhao, B. Feng, S. Chen, T. Gu, B. Yang and B. Jiang, *Chem. Commun.*, 2021, **57**, 4166–4169.
63 R. Barthos and F. Solymosi, *J. Catal.*, 2005, **235**, 60–68.
64 J. J. Spivey and G. Hutchings, *Chem. Soc. Rev.*, 2014, **43**, 792–803.
65 V. Fila, M. Bernauer, B. Bernauer and Z. Sobalik, *Catal. Today*, 2015, **256**, 269–275.
66 A. Samanta, X. Bai, B. Robinson, H. Chen and J. Hu, *Ind. Eng. Chem. Res.*, 2017, **56**, 11006–11012.
67 Q. Li, P. He, J. Jarvis, A. Bhattacharya, X. Mao, A. Wang, G. M. Bernard, V. K. Michaelis, H. Zeng, L. Liu and H. Song, *Appl. Catal., B*, 2018, **236**, 13–24.
68 A. Bhan and W. Nicholas Delgass, *Catal. Rev.: Sci. Eng.*, 2008, **50**, 19–151.
69 I. Vollmer, E. Abou-Hamad, J. Gascon and F. Kapteijn, *ChemCatChem*, 2020, **12**, 544–549.
70 M. Rahman, A. Sridhar and S. J. Khatib, *Appl. Catal., A*, 2018, **558**, 67–80.
71 V. Ramasubramanian, H. Ramsurn and G. L. Price, *J. Energy Chem.*, 2019, **34**, 20–32.
72 A. Sridhar, M. Rahman and S. J. Khatib, *ChemCatChem*, 2018, **10**, 2571–2583.
73 N. Pasupulety, A. A. Al-Zahrani, M. A. Daous, H. Driss and L. A. Petrov, *J. Mater. Res. Technol.*, 2021, **14**, 363–373.
74 T. S. Khan, S. Balyan, S. Mishra, K. K. Pant and M. A. Haider, *J. Phys. Chem. C*, 2018, **122**, 11754–11764.
75 I. Lezcano-González, R. Oord, M. Rovezzi, P. Glatzel, S. W. Botchway, B. M. Weckhuysen and A. M. Beale, *Angew. Chem., Int. Ed.*, 2016, **55**, 5215–5219.
76 J. Gao, Y. Zheng, J.-M. Jehng, Y. Tang, I. E. Wachs and S. G. Podkolzin, *Science*, 2015, **348**, 686–690.
77 M. A. Abedin, S. Kanitkar, S. Bhattar and J. J. Spivey, *Catal. Today*, 2021, **365**, 71–79.
78 H. Liu, H. Wang, A.-H. Xing and J.-H. Cheng, *J. Phys. Chem. C*, 2019, **123**, 15637–15647.
79 L. Ma and X. Zou, *Appl. Catal., B*, 2019, **243**, 703–710.
80 S. Fadaeerayeni, J. Shan, E. Sarnello, H. Xu, H. Wang, J. Cheng, T. Li, H. Toghiani and Y. Xiang, *Appl. Catal., B*, 2020, **601**, 117629.
81 A. Mehdad and R. F. Lobo, *Catal. Sci. Technol.*, 2017, **7**, 3562–3572.
82 D. Zeng, G. Zhu and C. Xia, *Fuel Process. Technol.*, 2022, **226**, 107087.
83 E. A. Belopukhov, D. I. Kir'yanov, M. D. Smolikov, V. A. Shkurenok, A. S. Belyi, A. V. Lavrenov, A. V. Kleimenov and D. O. Kondrashev, *Catal. Today*, 2021, **378**, 113–118.
84 V. Y. Tregubenko, K. V. Veretelnikov, N. V. Vinichenko, T. I. Gulyaeva, I. V. Muromtsev and A. S. Belyi, *Catal. Today*, 2019, **329**, 102–107.
85 D. Xu, B. Wu, P. Ren, S. Wang, C. Huo, B. Zhang, W. Guo, L. Huang, X. Wen, Y. Qin, Y. Yang and Y. Li, *Catal. Sci. Technol.*, 2017, **7**, 1342–1350.
86 W. D. Shafer, G. Jacobs, U. M. Graham, V. R. R. Pendyala, M. Martinelli, G. A. Thomas, T. Jermwongratanachai, A. MacLennan, Y. Hu and B. H. Davis, *Catal. Lett.*, 2018, **148**, 97–107.
87 T. E. Tshabalala and M. S. Scurrell, *Catal. Commun.*, 2015, **72**, 49–52.

88 A. Zaker, G. A. Tompsett, S. Wang, J. Q. Bond and M. T. Timko, *Fuel*, 2022, **310**, 122360.
89 C. Song, M. Y. Gim, Y. H. Lim and D. H. Kim, *Fuel*, 2019, **251**, 404–412.
90 G. Xu, P. Zhang, J. Cheng, L. Xu, J. Fan, X. Zhu and F. Yang, *Microporous Mesoporous Mater.*, 2022, **330**, 111494.
91 P. He, J. Jarvis, L. Liu and H. Song, *Fuel*, 2019, **239**, 946–954.
92 Q. Li, F. Zhang, J. Jarvis, P. He, M. M. Yung, A. Wang, K. Zhao and H. Song, *Fuel*, 2018, **219**, 331–339.
93 M. V. Luzgin, V. A. Rogov, S. S. Arzumanov, A. V. Toktarev, A. G. Stepanov and V. N. Parmon, *Catal. Today*, 2009, **144**, 265–272.
94 M. V. Luzgin, A. A. Gabrienko, V. A. Rogov, A. V. Toktarev, V. N. Parmon and A. G. Stepanov, *J. Phys. Chem. C*, 2010, **114**, 21555–21561.
95 P. He, A. Wang, S. Meng, G. M. Bernard, L. Liu, V. K. Michaelis and H. Song, *Catal. Today*, 2019, **323**, 94–104.
96 P. He, J. S. Jarvis, S. Meng, Q. Li, G. M. Bernard, L. Liu, X. Mao, Z. Jiang, H. Zeng, V. K. Michaelis and H. Song, *Appl. Catal., B*, 2019, **250**, 99–111.
97 M. Ellouh, Z. S. Qureshi, A. Aitani, M. N. Akhtar, Y. Jin, O. Koseoglu and H. Alasiri, *ChemistrySelect*, 2020, **5**, 13807–13813.
98 M. Ronda-Lloret, T. K. Slot, N. P. van Leest, B. de Bruin, W. G. Sloof, E. Batyrev, A. Sepúlveda-Escribano, E. V. Ramos-Fernandez, G. Rothenberg and N. R. Shiju, *ChemCatChem*, 2022, **14**, e202200446.
99 M. Ronda-Lloret, L. Yang, M. Hammerton, V. S. Marakatti, M. Tromp, Z. Sofer, A. Sepúlveda-Escribano, E. V. Ramos-Fernandez, J. J. Delgado, G. Rothenberg, T. Ramirez Reina and N. R. Shiju, *ACS Sustainable Chem. Eng.*, 2021, **9**, 4957–4966.
100 M. Ronda-Lloret, V. S. Marakatti, W. G. Sloof, J. J. Delgado, A. Sepúlveda-Escribano, E. V. Ramos-Fernandez, G. Rothenberg and N. R. Shiju, *ChemSusChem*, 2020, **13**, 6401–6408.
101 E. Devid, M. Ronda-Lloret, Q. Huang, G. Rothenberg, N. R. Shiju and A. Kleyn, *Chin. J. Chem. Phys.*, 2020, **33**, 243–251.
102 C. Brady, Q. Debruyne, A. Majumder, B. Goodfellow, R. Lobo, T. Calverley and B. Xu, *Chem. Eng. J.*, 2021, **406**, 127168.
103 N. Madaan, N. R. Shiju and G. Rothenberg, *Catal. Sci. Technol.*, 2016, **6**, 125–133.
104 S.-H. Chung, V. Lachman, T. K. Slot and N. R. Shiju, *Catal. Commun.*, 2023, **182**, 106754.
105 S. Shirazimoghaddam, I. Amin, J. A. Faria Albanese and N. R. Shiju, *ACS Eng. Au*, 2023, **3**, 37–44.
106 E. S. Gnanakumar, N. Chandran, I. V. Kozhevnikov, A. Grau-Atienza, E. V. Ramos Fernández, A. Sepulveda-Escribano and N. R. Shiju, *Chem. Eng. Sci.*, 2019, **194**, 2–9.
107 N. R. Shiju and V. V. Guliants, *ChemPhysChem*, 2007, **8**, 1615–1617.
108 E. V. Ramos-Fernandez, N. R. Shiju and G. Rothenberg, *RSC Adv.*, 2014, **4**, 16456–16463.